Ferromagnetic liquid thin films under applied field

S. Banerjee and M. Widom

Department of Physics, Carnegie Mellon University, Pittsburgh, Pennsylvania 15213

Theoretical calculations, computer simulations, and experiments indicate the possible existence of a ferromagnetic liquid state, although definitive experimental evidence is lacking. Should such a state exist, demagnetization effects would force a nontrivial magnetization texture. Since liquid droplets are deformable, the droplet shape is coupled with the magnetization texture. In a thin-film geometry in zero applied field, the droplet has a circular shape and a rotating magnetization texture with a point vortex at the center. We calculate the elongation and magnetization texture of such a ferromagnetic thin-film liquid droplet confined between two parallel plates under a weak applied magnetic field. The vortex stretches into a domain wall and exchange forces break the reflection symmetry. This behavior contrasts qualitatively and quantitatively with the elongation of paramagnetic thin films.

I. INTRODUCTION

The study of a possible ferromagnetic liquid state is a problem of considerable interest. In such a spontaneously magnetized liquid state, long range magnetic order would exist in the liquid without application of any external field. The existence of such a liquid state has been indicated by mean field calculations [1–5] and computer simulations on strongly polar fluids [6–9].

Experiments to observe ferromagnetism in liquids with strong magnetic interactions such as ferrofluids [10] have failed so far because the liquids freeze [11,12] or phase separate [13] well above the predicted low temperatures for the onset of spontaneous magnetization. Experiments on supercooled Co-Pd alloys [14] do indicate the possibility of ferromagnetism in liquids. In this case it is the strong exchange interaction and not the dipole interaction that would cause the spontaneous magnetization. The experimental evidence regarding Co-Pd is still not conclusive.

Although the existence of a ferromagnetic liquid state is yet to be confirmed experimentally, spontaneous polarization coupled with other order parameters has already been observed. Some electrically polarized liquid crystals [15] show a helical ordering of the dipole moments in the liquid. In superfluid ^{3}He the magnetic moment couples to the superconducting order parameter [16]. Many superfluid ^{3}He phases are therefore also magnetically ordered.

It is interesting to consider the magnetization texture (spatial variation of the orientation of magnetization) inside a droplet of such a ferromagnetic liquid [17]. The magnetization texture likes to avoid poles [18] to minimize its energy. However, this leads to defects inside the texture. For example, a rotating magnetization texture with cylindrical symmetry inside a sphere avoids all poles but has a vortex line running through the center. Near the vortex of such a texture the magnetization is topologically unstable [19] and might escape into the third dimension [20] with a nonzero component along the vortex line. Whether this happens depends on the balance between demagnetizing and vortex energies. Simulated annealing of the magnetization inside a cubic box suggests that replacing vortices with point defects may be

favorable [5]. Any defect is likely to have a system-shape-dependent energy cost causing a deformable liquid droplet to deviate from a spherical shape. The complete calculation of the shape of an unconfined ferromagnetic liquid droplet in three dimensions coupled with the calculation of its magnetization texture remains an unsolved problem.

This problem has a simple solution in two dimensions in zero field. The magnetization texture inside any soft (zero anisotropy) ferromagnetic solid thin film is given by van den Berg's algorithm [21] which avoids all poles, and thus all magnetostatic energy, at the expense of a domain wall through the film. A liquid droplet, which can change its shape, prefers a circular shape to minimize its surface energy. The magnetization lines inside a circle form concentric circles according to van den Berg's algorithm. For a circular shape the domain wall energy is also minimized because the domain wall shrinks to a point vortex. The circle thus solves the coupled texture and shape problem in zero field.

Our goal is to analyze the shape of a ferromagnetic liquid droplet under weak applied fields. Since the texture and shape of a three-dimensional drop are not precisely known at present, we concentrate on the two-dimensional case of a droplet confined between two parallel plates with spacing much smaller than the droplet diameter. When a field is applied parallel to the plates the magnetization texture distorts to exclude the magnetic field from the bulk of the droplet. Bryant and Suhl [22] calculated the texture of solid circular and elliptic thin films under applied field. We adapt their result to ferromagnetic liquids by letting the shape vary as the field is applied. We find that the droplet elongates to reduce its magnetostatic energy. The equilibrium shape is reached when the magnetostatic energy plus the surface energy is minimized.

In Sec. II we calculate elongation of a ferromagnetic thin film as a function of its undeformed radius, thickness, the saturation magnetization, and the applied field. In Sec. III A we contrast this behavior with that of paramagnetic thin films under applied fields and discuss why this contrasting behavior occurs. In Sec. II B we discuss the symmetry breaking of the droplet shape under exchange forces and its dependence on the applied field. Finally, Sec. IV summarizes our results.
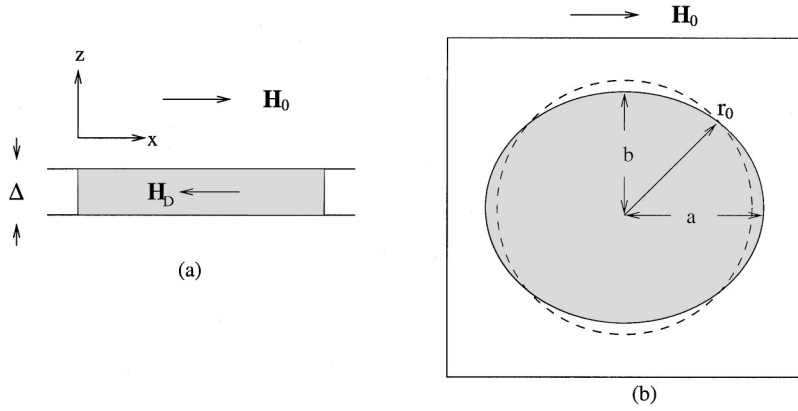
FIG. 1. (a) A side view of a ferromagnetic liquid droplet confined between two parallel plates. (b) A top view of the droplet elongating under applied field. The dashed line shows the undeformed droplet.

II. CALCULATION

Consider a homogeneous model liquid such that every point in the liquid has a saturation magnetization M_s with no anisotropy. Let a droplet of such a liquid in a spontaneously magnetized state be confined between two parallel plates as shown in Fig. 1(a). The spacing thickness Δ between the plates is kept much smaller than the diameter of the undeformed droplet so that the droplet has a very small aspect ratio $p \equiv \Delta/2r_0$. Figure 1(b) shows a droplet elongating under applied field. To a good approximation the droplet shape is an ellipse for small elongation. We define the elongation as

$$\epsilon \equiv a/b - 1, \tag{1}$$

where a and b are the semimajor and semiminor axes of the ellipse. We choose a coordinate system with the field in the $\hat{x}$ direction and $\hat{z}$ normal to the plates. The origin is at the center of the droplet.

Under zero external field this thin-film droplet has a circular shape. The magnetization texture $\mathbf{M}(\mathbf{r})$, given by van den Berg's algorithm [21], forms circles concentric with the droplet boundary. Because this texture is divergence-free and everywhere tangent to the surface, there are no magnetic poles [18] and hence no demagnetizing field. This texture therefore achieves the lowest possible magnetostatic energy. When an external field is applied, the circular magnetization texture distorts to reach a new equilibrium configuration. The new texture exhibits poles, making the magnetostatic energy shape dependent. The droplet elongates to reduce this shape-dependent magnetostatic energy and an equilibrium shape is reached when the magnetostatic plus surface energy is minimized. We neglect magnetic exchange energy because it is small relative to the magnetostatic energy, as discussed in Sec. III B. Our goal is to calculate this elongation as a function of the applied field and the various parameters for the droplet.

To calculate the magnetostatic energy of the droplet we make use of the calculations by Bryant and Suhl [22] for the magnetization texture of elliptic solid ferromagnetic thin films under applied field. Their calculations for the magnetization texture are for fixed shape. We let the shape of the thin-film droplet vary and calculate its energy as a function of the shape for small elongation. The elongation is then calculated by minimizing the total energy with respect to elongation.

Bryant and Suhl [22] calculate the equilibrium magnetization texture of an elliptical ferromagnetic thin film in applied field by drawing an analogy with the case of conductors in applied electric field. A ferromagnet is equivalent to a conductor because it has effectively an infinite permeability. When a conducting film is placed in an applied electric field, it expels the electric field by creating an induced charge density on its surface. A soft ferromagnet will similarly expel magnetic field if a magnetization texture can be found exhibiting the necessary surface pole density. These charges $\sigma_M(x,y)$ arise from the components of $\mathbf{M}$ normal to the top and bottom surfaces of the droplet and there are no poles within the bulk of the droplet,

$$\sigma_M(x,y) = \mathbf{M} \cdot \hat{\mathbf{n}},$$
$$\nabla \cdot \mathbf{M} = 0. \tag{2}$$

Here $\hat{\mathbf{n}}$ is the normal to the surface of the droplet. Solution for $\mathbf{M}$ inside the droplet satisfying Eq. (2) requires solving for $\mathbf{M}$ in three dimensions.

The problem can be reduced to two dimensions by noting that in the thin-film geometry ($\Delta/2r_0 \ll 1$), strong demagnetizing fields prevent the magnetization from tilting far out of the x-y plane. Therefore, the out-of-plane component of the magnetization M_z is nearly zero. Bryant and Suhl [22] define a new magnetization with $M_z = 0$, and treat the charge density $\sigma(x,y)$ as if it permeates through the film. The two-dimensional magnetization texture is defined by the pseudodivergence equation

$$\nabla \cdot \mathbf{M} \equiv \frac{\partial M_x}{\partial x} + \frac{\partial M_y}{\partial y} = -\rho_M = -\sigma_M(x,y)/\Delta. \tag{3}$$

The two-dimensional $\mathbf{M}$ solving Eq. (2) is a good approximation provided the film has a small aspect ratio ($\Delta/2r_0 \ll 1$). The partial differential equation (3) can be integrated, in principle, to find a solution for $\mathbf{M}(\mathbf{r})$ if it exists. Note that this solution for the two-dimensional magnetization texture does not satisfy Maxwell's equations because $\nabla \cdot \mathbf{M}$ does not vanish inside the droplet.

For an elliptic thin film, the charge density that expels the field can be calculated by solving Laplace's equation in ellipsoidal coordinates [23] and written in a convenient form as
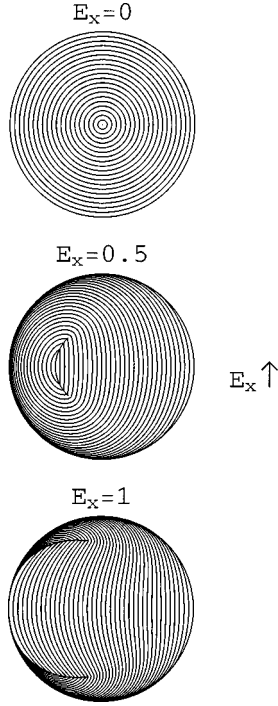
FIG. 2. The magnetization texture of a solid circular ferromagnetic thin film under applied field [22]. E_x is the reduced applied field defined in Eq. (5). The magnetization texture in zero field is going counterclockwise.

$$\sigma_M(x,y) = \frac{4M_s \Delta E_x x}{\pi a^2 [1-(x/a)^2-(y/b)^2]^{1/2}}, \quad (4)$$

where

$$E_x = H_0 \left(\frac{a^2-b^2}{8M_s b \Delta (\widetilde{K}-\widetilde{E})} \right) \quad (5)$$

is the reduced applied field. $\widetilde{K}$ and $\widetilde{E}$ are complete elliptic integrals of the first and second kind, respectively, of the argument $(1-b^2/a^2)^{1/2}$. For $E_x \le 1$, Eq. (3) can be integrated to find the magnetization texture that expels the magnetic field. A C-shaped domain wall (see Fig. 2) appears inside the droplet for nonzero field. For $E_x > 1$, the domain wall intersects the boundary of the film and the field penetrates the interior of the film.

We use this result to calculate the magnetostatic energy of a liquid droplet. Since the above calculations are for zero anisotropy, they also apply to liquids. We begin with the general expression for the total magnetostatic energy of any magnetization distribution under an applied field,

$$E_M = -\int d\tau \mathbf{H}_0 \cdot \mathbf{M} - \tfrac{1}{2} \int d\tau \mathbf{H}_D \cdot \mathbf{M}. \quad (6)$$

The first term on the right hand side of Eq. (6) is the energy of the applied field $\mathbf{H}_0$ acting on magnetization $\mathbf{M}$. The second term is the self-energy (hence the factor of $\tfrac{1}{2}$) due to the magnetization interacting with its own demagnetizing field $\mathbf{H}_D$. For $E_x \le 1$, $\mathbf{H}_D = -\mathbf{H}_0$ because the magnetization expels the field, and therefore the magnetostatic energy

$$E_M = -\tfrac{1}{2} \int d\tau \mathbf{H}_0 \cdot \mathbf{M}. \quad (7)$$

Using $\rho_M = -\boldsymbol{\nabla} \cdot \mathbf{M}$, writing $\mathbf{H}_0 = -\boldsymbol{\nabla} \phi_0$, and integrating by parts, the magnetostatic energy in Eq. (7) can be rewritten as

$$E_M = \tfrac{1}{2} \int d\tau \, \phi_0 \rho_M, \quad (8)$$

where $\phi_0 = -H_0 x$ is the potential due to $\vec{H}_0$. Using $\rho_M = \sigma_M / \Delta$ and Eqs. (4) and (5) and calculating the integral in Eq. (8) gives

$$E_M = -\frac{32}{3} E_x^2 M_s^2 \Delta^2 a b^2 \frac{\widetilde{K}-\widetilde{E}}{a^2-b^2} = -\frac{1}{6} H_0^2 a \frac{a^2-b^2}{\widetilde{K}-\widetilde{E}}, \quad (9)$$

Assume that the applied field is small so that $\epsilon \ll 1$. Expanding the result in Eq. (9) for small ϵ gives

$$E_M = -\frac{2H_0^2 r_0^3}{3\pi} (1+\tfrac{3}{4}\epsilon), \quad (10)$$

with corrections of higher order in ϵ and higher order in the aspect ratio $\Delta/2r_0$. As expected, the leading correction to the energy is negative, so the droplet elongates to reduce its magnetostatic energy. Interestingly, the magnetostatic energy is independent of the saturation magnetization M_s. This is so because, as long as $E_x \le 1$, the charge density ρ_M does not depend on M_s. The factor of M_s in the numerator of $\sigma_M(x,y)$ in Eq. (4) cancels against the factor of M_s in the denominator of E_x in Eq. (5). Physically, the charge density of a given distribution is proportional to M_s, but the distortion that creates ρ_M varies inversely with M_s.

The magnetostatic energy is also independent of Δ to the lowest order in the aspect ratio $\Delta/2r_0$. To understand this, note that the expression for the reduced applied field E_x has a factor Δ in the denominator implying that thicker films can expel higher values of applied field for a given distortion. Thus a thicker film has a smaller distortion in its texture, for a particular value of applied field, than a thinner film. This is confirmed by the factor of Δ in the denominator of the charge density ρ_M. When the energy density is integrated over the volume it yields a magnetostatic energy independent of Δ.

As the droplet elongates, its perimeter increases and is given by

$$S = 2\pi r_0 (1+\tfrac{3}{16}\epsilon^2), \quad (11)$$

with higher order corrections in ϵ. The variation of the perimeter is quadratic in ϵ as expected because the perimeter should increase regardless of the sign of ϵ. Since the area of the droplet in contact with the plates remains constant, the relevant surface energy is the surface energy along the perimeter,

$$E_S = \sigma S \Delta, \quad (12)$$

where σ is the surface tension along the perimeter of the droplet. Note that we consider the case of 90° contact angle
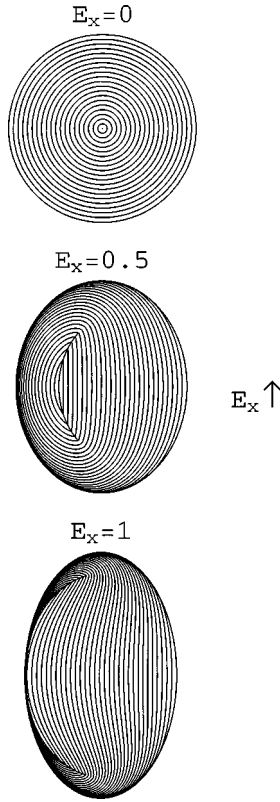
FIG. 3. The magnetization texture of a liquid ferromagnetic thin film elongating under applied field. The magnetization texture in zero field is going counterclockwise. Values for dimensionless field h^* [see Eq. (16)] are 0, 0.42, and 0.68.

of the magnetic fluid–nonmagnetic fluid interface with the boundary plates. Discussion of surface energy for other contact angles is in Ref. [24].

Minimizing the total energy $E_M + E_S$ with respect to ϵ gives the elongation of a ferromagnetic droplet,

$$\epsilon_{\text{ferro}} = \frac{2H_0^2 r_0^2}{3\pi^2 \sigma \Delta}. \tag{13}$$

The elongation is quadratic in the applied field since reversing the field direction should not affect the result. At fixed thickness Δ, droplets with larger radius r_0 will elongate more. This is because the magnetostatic energy in Eq. (10) is proportional to r_0^3, whereas the surface energy is proportional to the area of the curved surface (of order $r_0\Delta$). The elongation, however, is inversely proportional to Δ. This is because the droplets with larger thickness find it easier to expel the applied field. The same applied field causes a relatively smaller distortion in the magnetization texture of a thicker droplet, and a smaller distortion of texture causes a smaller elongation. Figure 3 shows the magnetization texture of a droplet as it elongates under applied field.

Determining the applied field at which the domain wall touches the boundary and field penetration occurs is complicated by the dependence of the reduced field E_x, defined in Eq. (5), on elongation. Basically, a given applied field $\mathbf{H}_0$ causes a greater distortion of the magnetization texture in a droplet that is elongated in the field direction than it would have caused in a circular droplet. This is because the demag-

netizing field becomes weak in elongated droplets (that is why the droplet elongates, after all) so a larger charge density is needed to achieve a demagnetizing field $\mathbf{H}_D = -\mathbf{H}_0$. Correspondingly, a lower applied field is needed to achieve penetration for an elongated droplet than for a circular droplet.

The reduced applied field in Eq. (5) can be written to first order in ϵ as

$$E_x = \frac{H_0 r_0}{2\pi \Delta M_s} (1 + \tfrac{3}{4}\epsilon), \tag{14}$$

with corrections of order ϵ^3. Substituting the expression for elongation Eq. (13) into the above gives

$$E_x = \frac{H_0 r_0}{2\pi \Delta M_s} \left(1 + \frac{H_0^2 r_0^2}{2\pi^2 \Delta \sigma} \right). \tag{15}$$

For any finite σ, E_x now depends nonlinearly on H_0. E_x is still a useful quantity as it measures the distortion in the magnetization texture of the droplet, but its relation to the applied field is nontrivial. It is therefore convenient to define a new dimensionless field,

$$h^* \equiv \frac{H_0 r_0}{2\pi \Delta M_s}, \tag{16}$$

that equals E_x when the droplet is circular. We also define a dimensionless surface tension

$$\sigma^* = \frac{\sigma}{2M_s^2 \Delta}, \tag{17}$$

so that the reduced field can be written as

$$E_x = h^* \left(1 + \frac{h^{*2}}{\sigma^*} \right). \tag{18}$$

Our calculations hold in the limit of small droplet distortion, $h^{*2}/\sigma^* \ll 1$, and nonpenetration of the field, $E_x < 1$. Consider the applied field at which field penetration occurs. Solving Eq. (18) for the critical applied field h_c^* for which $E_x = 1$ yields $h_c^* \approx 1 - 1/\sigma^*$ in the limit of nearly undeformable droplets, $\sigma^* \gg 1$.

Figure 3 illustrates the simultaneous evolution of droplet shape and texture. Three stages are shown, at $E_x = 0$, 0.5, and 1. Parameters are chosen so that $\sigma^* = 1$. As expected, in contrast to the values of E_x, the actual applied field values h^* become more closely spaced as the elongation grows, and $h_c^* = 0.68 < 1$.

III. DISCUSSION

A. Contrast with paramagnetic thin films

Expression (13) for elongation of ferromagnetic droplets contrasts with the elongation of paramagnetic droplets in the same thin-film geometry. For a paramagnetic thin film with susceptibility χ, the elongation has been previously calculated [24],
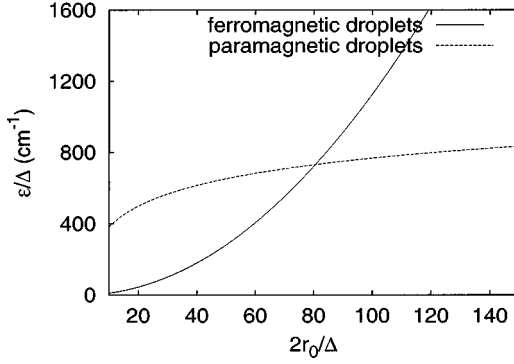
FIG. 4. Plots of ϵ/Δ vs $2r_0/\Delta$ for ferromagnetic and paramagnetic droplets for a fixed value of $H_0 = 20$ G.

$$\epsilon_{\text{para}} = \frac{\chi^2 H_0^2 \Delta}{\sigma} \ln \frac{Cr_0}{\Delta}, \qquad (19)$$

where C is a constant.

To understand this contrasting behavior we provide the following simple argument on dimensional grounds. The elongation is a ratio of the magnetostatic and surface energies. Let Q be the net charge on the portion of the droplet with $x > 0$. For $x < 0$ the net charge is $-Q$. In both the ferromagnetic and paramagnetic cases, the charges on average are separated by distances of order r_0, and therefore the magnetostatic energy varies as Q^2/r_0. Dividing this by the surface energy (of order $r_0 \Delta \sigma$) gives the elongation

$$\epsilon \sim \frac{Q^2}{r_0^2 \sigma \Delta}, \qquad (20)$$

where ''$\sim$'' indicates proportionality. In the case of a ferromagnetic droplet $Q \sim H_0 r_0^2$ because the charge density ρ_M is distributed in the bulk of the droplet (volume $\sim r_0^2 \Delta$) but is inversely proportional to Δ. This explains why the elongation of a ferromagnetic droplet increases rapidly with r_0 and decreases with Δ in Eq. (13). In the case of a paramagnetic droplet, the charges are distributed mainly along the curved surface of the droplet, so the total charge Q is proportional to $\chi H_0 r_0 \Delta$. Our simple dimensional argument gives $\epsilon \sim \chi^2 H_0^2 \Delta/\sigma$, which reproduces Eq. (19) except for the dimensionless $\ln(r_0/\Delta)$, and explains why the elongation in the paramagnetic case depends only weakly on r_0 and increases strongly with Δ.

Although theory and computer simulations predict the existence of a ferromagnetic liquid state there is still not much experimental evidence for it. The contrasting behavior of ferromagnetic thin films and paramagnetic thin films under applied fields could serve as a useful test to detect such a state. This contrasting behavior can be neatly captured in a picture if one plots ϵ/Δ vs the inverse aspect ratio $2r_0/\Delta$ at a fixed field value. Figure 4 shows such a plot for experiments on ferromagnetic and paramagnetic droplets of a hypothetical fluid at $H_0 = 20$ G. The fluid has a susceptibility $\chi = 5$ in the paramagnetic phase, surface tension $\sigma = 60$ dynes/cm, and $M_s = 500$ G, typical of ferrofluids. We take the droplet dimensions $2r_0 = 120 \, \mu$m and $\Delta = 1.2 \, \mu$m so that $p = 2r_0/\Delta = 10^{-2}$ and $\sigma^* = 1$. The value $H_0 = 20$ G corresponds to h^*

$= 0.16$ for the droplet in the ferromagnetic phase. Recall that for $\sigma^* = 1$ field penetration occurs at $h^* = 0.68$.

B. Symmetry breaking of shape under exchange interaction

Despite the asymmetric magnetization texture, the droplet shape in Fig. 3 has reflection symmetry about the field direction. Interactions of the magnetic poles with the applied field and with each other create the forces that deform the droplet. Since for a symmetric shape the induced charge density is symmetric, the droplet deformation is symmetric. The deformed magnetization texture is asymmetric because the direction of rotation of magnetization lines (counterclockwise in Figs. 2 and 3) breaks the left-right symmetry. If the exchange interaction due to spatial variation of magnetization were to be included, the droplet shape would become asymmetric to lower its exchange energy.

For an isotropic medium, the exchange energy density can be written as [25]

$$U_{\text{ex}} = \frac{1}{2} \alpha \frac{\partial M_k}{\partial x_i} \frac{\partial M_k}{\partial x_i}, \qquad (21)$$

where α is the exchange constant and the summation convention is employed. The magnetization texture for a droplet under applied field breaks the left-right symmetry (see Figs. 2 and 3). The breaking of the symmetry is most evident at the domain wall where U_{ex} is singular. The exchange interaction creates forces that break the left-right symmetry of the droplet shape.

The main contribution to the exchange energy of the droplet comes from near the domain wall, where the magnetization has an apparent discontinuity of order M_s. The domain wall actually spreads to a finite width w to lower its exchange energy at the cost of acquiring a demagnetizing energy. Since the magnetization changes by an amount of order M_s over a distance w, the domain wall exchange energy density is roughly $\alpha M_s^2/w^2$. For a Bloch domain wall [26] with $w \ll \Delta$ the demagnetizing energy density is of order $M_s^2 w/\Delta$. Minimizing the total energy per unit domain wall length with respect to the width gives w of order $(\alpha \Delta)^{1/3}$ and energy density of order $\alpha^{1/3} M_s^2/\Delta^{2/3}$.

For $E_x \ll 1$, symmetry arguments and numerical calculations suggest that domain wall arclength varies as $E_x^2 r_0$. The total energy of the domain wall can be estimated by multiplying the domain wall energy density by the domain wall arclength ($E_x^2 r_0$) and cross section ($w\Delta$) to get

$$E_{\text{wall}} \sim \alpha^{2/3} M_s^2 E_x^2 \Delta^{2/3} r_0 = \alpha^{2/3} H_0^2 \frac{r_0^3}{\Delta^{4/3}}. \qquad (22)$$

The ratio of the domain wall energy to the magnetostatic energy (10) varies as $(\alpha/\Delta^2)^{2/3}$. Therefore, the relative importance of exchange effects diminishes for large thickness Δ.

To understand how exchange interaction breaks the symmetry of the shape, we analyze the exchange forces on a circular disk in an applied field (Fig. 2). We write the shape of the droplet as a perturbed circle breaking the left-right symmetry,

$$r(\theta) = r_0 \left(1 - \frac{\psi^2}{2} + \psi \sin 3\theta \right). \qquad (23)$$

Here θ is the angle measured counterclockwise from the direction of the applied field in the plane of the droplet. The sin 3θ term is the lowest harmonic in θ that breaks the left-right symmetry of the shape. The perturbation keeps the area constant to ensure that the volume of the droplet does not change. Assuming analytic variation with respect to the perturbation and the applied field, the domain wall energy takes the following form for small ψ and E_x:

$$E_{\text{wall}} = \alpha^{2/3} M_s^2 E_x^2 r_0 \Delta^{2/3} (A + B\psi E_x), \qquad (24)$$

where A and B are dimensionless constants. The order ψ term is multiplied by E_x because under simultaneous reversals of ψ and E_x the domain wall energy remains the same.

The surface energy of the droplet varies quadratically with ψ,

$$E_s = 2\pi r_0 \Delta \sigma (1 + 2\psi^2). \qquad (25)$$

The magnetostatic energy (10) of the droplet has an order ψ^2 correction that can be neglected because it is higher order in the applied field. Minimizing $E_S + E_{\text{wall}}$ with respect to ψ gives

$$\psi = -\frac{B\alpha^{2/3} M_s^2 E_x^3 r_0}{8\pi\Delta^{1/3}\sigma}. \qquad (26)$$

We conclude that for weak applied fields the symmetry breaking in shape will be much smaller than the elongation of the droplet, which varies as E_x^2. The direction of symmetry breaking (sign of ψ) remains undetermined, since it depends on the sign of B. We expect the direction of symmetry breaking to shorten the length of the domain wall.

IV. CONCLUSION

We calculate the magnetization texture and elongation of a ferromagnetic thin film under weak applied fields. The point vortex favored at zero field elongates into a curved domain wall in an applied field. We find that the droplet elongation is proportional to the square of the radius of the undeformed droplet and inversely proportional to its thickness. When domain wall energies are considered, the ferromagnetic droplet may break reflection symmetry. These results contrast with those of paramagnetic thin films. We propose this different behavior under applied field as one possible way to detect the ferromagnetic state in a liquid.

ACKNOWLEDGMENTS

[1] K. Sano and M. Doi, J. Phys. Soc. Jpn. **52**, 2810 (1983).

[2] A. O. Tsebers, Magnetohydrodynamics **2**, 42 (1982).

[3] H. Zhang and M. Widom, J. Magn. Magn. Mater. **122**, 119 (1993); Phys. Rev. E **49**, R3591 (1994).

[4] B. Groh and S. Dietrich, Phys. Rev. Lett. **72**, 2422 (1994); **74**, 2617 (1995); Phys. Rev. E **50**, 3814 (1994).

[5] B. Groh and S. Dietrich, Phys. Rev. E **57**, 4535 (1998).

[6] D. Wei and G. N. Patey, Phys. Rev. Lett. **68**, 2043 (1992); Phys. Rev. A **46**, 7783 (1992).

[7] J. J. Weis, D. Levesque, and G. J. Zarragoicoechea, Phys. Rev. Lett. **69**, 913 (1992).

[8] J. J. Weis and D. Levesque, Phys. Rev. E **48**, 3728 (1993).

[9] M. J. Stevens and G. S. Grest, Phys. Rev. E **51**, 5962 (1995); **51**, 5976 (1995).

[10] R. E. Rosensweig, *Ferrohydrodynamics* (Cambridge University Press, Cambridge, England, 1985).

[11] J. Zhang, C. Boyd, and W. Luo, Phys. Rev. Lett. **77**, 390 (1996).

[12] D. Ederbeck and H. Ahlers, J. Magn. Magn. Mater. **192**, 148 (1999).

[13] W. Luo, Nuovo Cimento D **16**, 1199 (1994).

[14] J. Reske, D. M. Herlach, F. Keuser, K. Maier, and D. Platzek, Phys. Rev. Lett. **75**, 737 (1995); T. Albrecht, C. Buhrer, M. Fahnle, K. Maier, D. Platzek, and J. Reske, Appl. Phys. A: Mater. Sci. Process. **65**, 215 (1997).

[15] R. B. Meyer, L. Liebert, L. Strzelecki, and P. Keller, J. Phys. (France) Lett. **30**, 69 (1975).

[16] N. D. Mermin and D. M. Lee, Sci. Am. **235**, 56 (1976).

[17] P. G. de Gennes and P. A. Pincus, Solid State Commun. **7**, 339 (1969).

[18] W. F. Brown, *Magnetostatic Principles in Ferromagnetism* (North-Holland, Amsterdam, 1962).

[19] N. D. Mermin, Rev. Mod. Phys. **51**, 591 (1979).

[20] A. Hubert, J. Phys. (Paris) Colloq. **8**, 1859 (1988).

[21] H. A. M. van den Berg, J. Appl. Phys. **60**, 1104 (1986).

[22] P. Bryant and H. Suhl, Appl. Phys. Lett. **54**, 2224 (1989).

[23] The expression for $\sigma_M(x,y)$ appears in Ref. [22]. See Ref. [25], Sec. 4, and J. H. Jeans, *The Mathematical Theory of Electricity and Magnetism*, 5th ed. (Cambridge University Press, Cambridge, England, 1958), Sec. 295, for discussion of similar problems.

[24] S. Banerjee, M. Fasnacht, S. Garoff, and M. Widom, Phys. Rev. E **60**, 4272 (1999).

[25] L. D. Landau and E. M. Lifshitz, *Electrodynamics of Continuous Media* (Pergamon, Oxford, 1984).

[26] See S. Middelhoek, J. Appl. Phys. **34**, 1054 (1963) for a review article on domain walls in ferromagnetic thin films.